Coupled Systems Mechanics, *Vol. 5, No. 3 (2016) 269-283*
DOI: https://doi.org/10.12989/csm.2016.5.3.269

Bending analysis of an imperfect advanced composite plates resting on the elastic foundations

Tahar Hassaine Daouadji*[1,2], Rabia Benferhat[3] and Belkacem Adim[1,2]

[1]*Département de génie civil, Université Ibn Khaldoun Tiaret, BP 78 Zaaroura, 14000 Tiaret, Algérie*
[2]*Laboratoire de Géomatique et Développement Durable, Université Ibn Khaldoun de Tiaret, Algérie*
[3]*Laboratoire de Géo-matériaux, Département de Génie Civil, Université de Chlef 02000, Algérie*

(Received September 10, 2016, Revised December 17, 2016, Accepted January 25, 2017)

Abstract. A two new high-order shear deformation theory for bending analysis is presented for a simply supported, functionally graded plate with porosities resting on an elastic foundation. This porosities may possibly occur inside the functionally graded materials (FGMs) during their fabrication, while material properties varying to a simple power-law distribution along the thickness direction. Unlike other theories, there are only four unknown functions involved, as compared to five in other shear deformation theories. The theories presented are variationally consistent and strongly similar to the classical plate theory in many aspects. It does not require the shear correction factor, and gives rise to the transverse shear stress variation so that the transverse shear stresses vary parabolically across the thickness to satisfy free surface conditions for the shear stress. It is established that the volume fraction of porosity significantly affect the mechanical behavior of thick function ally graded plates. The validity of the two new theories is shown by comparing the present results with other higher-order theories. The influence of material parameter, the volume fraction of porosity and the thickness ratio on the behavior mechanical P-FGM plate are represented by numerical examples.

Keywords: functionally graded material; higher-order theory; volume fraction of porosity; Winkler-Pasternak elastic foundation

1. Introduction

An ideal material combines the best properties of metals and ceramics-the toughness, electrical conductivity, and machinability of metals, and the low density, high strength, high stiffness, and temperature resistance of ceramics. Graded materials are also required to adhere two different materials in structures subjected to different loading environments (Chakraborty 2003). The functionally graded materials (FGMs) (Koizumi 1993, Suresh 1998), a new generation of advanced inhomogeneous composite materials first proposed for thermal barriers (Koizumi 1997), have been increasingly applied for modern engineering structures in the extremely high temperature environment. Plates supported by elastic foundations have been widely adopted by many researchers to model various engineering problems during the past decades. To describe

*Corresponding author, Professor, E-mail: daouadjitah@yahoo.fr

http://www.techno-press.com/journals/csm&subpage=7 ISSN: 2383-8477 (Print), 2466-0523 (Online)

the interactions of the plate and foundation as more appropriate as possible, scientists have proposed various kinds of foundation models (Kerr 1964).

The simplest model for the elastic foundation is the Winkler model, which regards the foundation as a series of separated springs without coupling effects between each other, resulting in the disadvantage of discontinuous deflection on the interacted surface of the plate. This was later improved by Pasternak (Pasternak 1954) who took account of the interactions between the separated springs in the Winkler model by introducing a new dependent parameter. From then on, the Pasternak model was widely used to describe the mechanical behavior of structure-foundation interactions (Xiang 1994, Zhou 2004, Ait Amar 2015, Bellifa 2015, Gafour 2015, Baghdadi 2015, Naceri 2012, Mantari 2014). As the application of FGMs increases, new methodologies have to be developed to characterize them, and to design and analyze structural components made of these materials. The literature on the response of FGM plates resting on the elastic foundations to mechanical and other loadings are limited. Zenkour (2010) studied the effect of the Hygro-thermo-mechanical on FGM plates resting on elastic foundations, the elastic coefficients, thermal coefficient and moisture expansion coefficient of the plate are assumed to be graded in the thickness direction. Shen (2010) has analyzed a nonlinear bending for of FGM plates subjected to combined loading and resting on elastic foundations. Pradhan (2009) studied the thermo-mechanical vibration of functionally graded (FG) beams and functionally graded sandwich under variable elastic foundations using differential quadrature method. Meksi *et al*. (2015) proposed a simple shear deformation theory based on neutral surface position for functionally graded plates resting on Pasternak elastic foundations. However, in FGM fabrication, micro voids or porosities can occur within the materials during the process of sintering. This is because of the large difference in solidification temperatures between materials constituents (Zhu *et al*. 2001, Abdelhak 2015, Bourada 2015, Hamidi 2015, Boumia 2014, Bouazza 2015, Bensatallah 2016, Zidour 2014, Mahi 2015). Wattanasakulpong *et al*. (2012) also gave the discussion on porosities happening inside FGM samples fabricated by a multi-step sequential in filtration technique. Therefore, it is important to take into account the porosity effect when designing FGM structures subjected to dynamic loadings.

In this study, a two new refined theory for bending analysis of simply supported FGM plates with considering porosities that may possibly occur inside the functionally graded materials (FGMs) during their fabrication and resting on the elastic foundations are proposed. The plates are made of an isotropic material with material properties varying in the thickness direction only. Numerical examples are presented to illustrate the accuracy and efficiency of the two present theories and the influence of material parameter, the volume fraction of porosity and the thickness ratio on the behavior mechanical FGM plate.

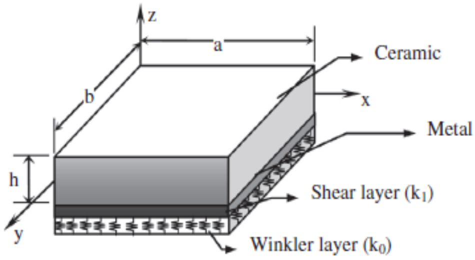

Fig. 1 Geometry and coordinates of considered FG plate which is resting on elastic foundation

2. Mathematical model and governing equations

2.1 Geometrical configuration

In the present study, a functionally graded simply supported rectangular plate which has the uniform thickness, the length a, and the width b is considered (Fig. 1). It is assumed to be rested on a Winkler-Pasternak type elastic foundation with the Winkler stiffness of k_0 and shear stiffness of k_1.

2.2 Material properties

A FG plate made from a mixture of two material phases, for example, a metal and a ceramic. The material properties of FG plates are assumed to vary continuously through the thickness of the plate. In this investigation, the imperfect plate is assumed to have porosities spreading within the thickness due to defect during production. Consider an imperfect FGM with a porosity volume fraction, $\alpha(\alpha<<1)$, distributed evenly among the metal and ceramic, the modified rule of mixture proposed by Wattanasakulpong and Ungbhakorn (2014) is used as

$$P = P_m(V_m - \frac{\alpha}{2}) + P_c(V_c - \frac{\alpha}{2}) \tag{1}$$

Now, the total volume fraction of the metal and ceramic is: $V_m+V_c=1$, and the power law of volume fraction of the ceramic is described as

$$V_c = (\frac{z}{h} + \frac{1}{2})^p \tag{2}$$

Hence, all properties of the imperfect FGM can be written as

$$P = (P_c - P_m)(\frac{z}{h} + \frac{1}{2})^p + P_m - (P_c + P_m)\frac{\alpha}{2} \tag{3}$$

It is noted that the positive real number k ($0 \leq P < \infty$) is the power law or volume fraction index, and z is the distance from the mid-plane of the FG plate. The FG plate becomes a fully ceramic plate when k is set to zero and fully metal for large value of k.

Thus, the Young's modulus (E) and material density (ρ) equations of the imperfect FGM plate can be expressed as

$$\begin{aligned} E(z) &= (E_c - E_m)(\frac{z}{h} + \frac{1}{2})^p + E_m - (E_c + E_m)\frac{\alpha}{2} \\ \rho(z) &= (\rho_c - \rho_m)(\frac{z}{h} + \frac{1}{2})^p + \rho_m - (\rho_c + \rho_m)\frac{\alpha}{2} \end{aligned} \tag{4}$$

However, Poisson's ratio (v) is assumed to be constant. The material properties of a perfect FG plate can be obtained when α is set to zero.

2.3 Fundamental formulations

2.3.1 Higher-order plate theory

Basic assumptions for the displacement field of the plate are given as below

$$\begin{aligned} u(x,y,z) &= u_0(x,y) - z\frac{\partial w_0}{\partial x} + \Psi(z).\theta_x \\ v(x,y,z) &= v_0(x,y) - z\frac{\partial w_0}{\partial y} + \Psi(z).\theta_y \\ w(x,y,z) &= w_0(x,y) \end{aligned} \tag{5}$$

Where u, v, w are displacements in the x, y, z directions, u_0, v_0 and w_0 are midplane displacements, and θ_x and θ_y are the rotations of normal's to the midplane about the y and x axes, respectively. $\psi(z)$ represents shape function determining the distribution of the transverse shear strains and stresses along the thickness. The displacement field of the classical thin plate theory (CPT) is obtained easily by setting $\psi(z)=0$. The displacement of the first-order shear deformation plate theory (FSDPT) is obtained by setting $\psi(z)=z$. Also, the displacement of parabolic shear deformation plate theory of Reddy (1984) is obtained by setting

$$\Psi(z)=z\left(1-\frac{4z^2}{3h^2}\right) \tag{6a}$$

$$\Psi(z)=z\left(1-\frac{4z^2}{3h^2}\right) \tag{6b}$$

In addition, the exponential shear deformation plate theory of Karama (2003) is obtained by setting

$$\Psi(z)=ze^{-2\left(\frac{z}{h}\right)^2} \tag{6c}$$

2.3.2 Present refined sinusoidal shear deformation plate theory

Unlike the other theories, the number of unknown functions involved in the two present refined plate theory is only four, as against five in case of other shear deformation theories (Reddy 1984, Karama *et al*. 2003). The theory presented is variationally consistent, does not require shear correction factor, and gives rise to transverse shear stress variation such that the transverse shear stresses vary parabolically across the thickness satisfying shear stress free surface conditions.

Basic assumptions

Assumptions of the present refined plate theory are as follows:

• The displacements are small in comparison with the plate thickness and, therefore, strains involved are infinitesimal.

• The transverse displacement W includes two components of bending w_b, and shear w_s. These components are functions of coordinates x, y, and time t only.

$$w(x,y,z)=w_b(x,y)+w_s(x,y) \tag{7a}$$

• The transverse normal stress σ_z is negligible in comparison with in-plane stresses σ_x and σ_y.

• The displacements U in x direction and V in y direction consist of extension, bending, and shear components.

$$u=u_0+u_b+u_s \qquad v=v_0+v_b+v_s \tag{7b}$$

The shear components u_s and v_s give rise, in conjunction with w_s, to the parabolic variations of shear strains γ_{xz}, γ_{yz} and hence to shear stresses τ_{xz}, τ_{yz} through the thickness of the plate in such a way that shear stresses τ_{xz}, τ_{yz} are zero at the top and bottom faces of the plate. Consequently, the expression for us and v_s can be given as

$$u_s=-\left(z-\sin\left(\frac{\pi z}{h}\right)\right)\frac{\partial w_s}{\partial x} \qquad v_s=-\left(z-\sin\left(\frac{\pi z}{h}\right)\right)\frac{\partial w_s}{\partial y} \tag{7c}$$

Displacement fields and strains

The assumed displacement field is as follows

$$
\begin{aligned}
u(x,y,z) &= u_0(x,y) - z\frac{\partial w_b}{\partial x} - f(z)\frac{\partial w_s}{\partial x} \\
v(x,y,z) &= v_0(x,y) - z\frac{\partial w_b}{\partial y} - f(z)\frac{\partial w_s}{\partial y} \\
w(x,y,z) &= w_b(x,y) + w_s(x,y)
\end{aligned}
\tag{8}
$$

Where u_0 and v_0 are the mid-plane displacements of the plate in the x and y direction, respectively; w_b and w_s are the bending and shear components of transverse displacement, respectively, while $f(z)$ represents shape functions determining the distribution of the transverse shear strains and stresses along the thickness and is given as

Theory 01 (Benferhat *et al*. 2015)

$$f(z) = z - \sin\left(\frac{\pi z}{h}\right) \tag{9a}$$

Theory 02 (Daouadji *et al*. 2012)

$$f(z) = \frac{3\pi}{2}h.\tanh\left(\frac{z}{h}\right) - \frac{3\pi}{2}z.\sec h^2\left(\frac{1}{2}\right) + z \tag{9b}$$

It should be noted that unlike the first-order shear deformation theory, this theories does not require shear correction factors. The kinematic relations can be obtained as follows

$$
\begin{aligned}
\varepsilon_x &= \varepsilon_x^0 + z\,k_x^b + f(z)\,k_x^s \\
\varepsilon_y &= \varepsilon_y^0 + z\,k_y^b + f(z)\,k_y^s \\
\gamma_{xy} &= \gamma_{xy}^0 + z\,k_{xy}^b + f(z)\,k_{xy}^s \\
\gamma_{yz} &= g(z)\,\gamma_{yz}^s \\
\gamma_{xz} &= g(z)\,\gamma_{xz}^s \\
\varepsilon_z &= 0
\end{aligned}
\tag{10}
$$

Where

$$
\begin{gathered}
\varepsilon_x^0 = \frac{\partial u_0}{\partial x},\quad k_x^b = -\frac{\partial^2 w_b}{\partial x^2},\quad k_x^s = -\frac{\partial^2 w_s}{\partial x^2},\quad \varepsilon_y^0 = \frac{\partial v_0}{\partial y},\quad k_y^b = -\frac{\partial^2 w_b}{\partial y^2},\quad k_y^s = -\frac{\partial^2 w_s}{\partial y^2} \\
\gamma_{xy}^0 = \frac{\partial u_0}{\partial y} + \frac{\partial v_0}{\partial x},\quad k_{xy}^b = -2\frac{\partial^2 w_b}{\partial x \partial y},\quad k_{xy}^s = -2\frac{\partial^2 w_s}{\partial x \partial y},\quad \gamma_{yz}^s = \frac{\partial w_s}{\partial y},\quad \gamma_{xz}^s = \frac{\partial w_s}{\partial x},\quad g(z) = 1 - f'(z),\quad f'(z) = \frac{df(z)}{dz}
\end{gathered}
\tag{11}
$$

For elastic and isotropic FGMs, the constitutive relations can be written as

$$
\begin{gathered}
\begin{Bmatrix} \sigma_x \\ \sigma_y \\ \tau_{xy} \end{Bmatrix} = \begin{bmatrix} Q_{11} & Q_{12} & 0 \\ Q_{12} & Q_{22} & 0 \\ 0 & 0 & Q_{66} \end{bmatrix} \begin{Bmatrix} \varepsilon_x \\ \varepsilon_y \\ \gamma_{xy} \end{Bmatrix} \\
\begin{Bmatrix} \tau_{yz} \\ \tau_{zx} \end{Bmatrix} = \begin{bmatrix} Q_{44} & 0 \\ 0 & Q_{55} \end{bmatrix} \begin{Bmatrix} \gamma_{yz} \\ \gamma_{zx} \end{Bmatrix}
\end{gathered}
\tag{12}
$$

Where (σ_χ, τ_y, $\tau_{\chi y}$, $\tau_{\chi z}$, τ_{yz}) and (ε_χ, ε_y, $\gamma_{\chi y}$, $\gamma_{\chi z}$, γ_{yz}) are the stress and strain components, respectively. Stiffness coefficients, Q_{ij} can be expressed as

$$Q_{11} = Q_{22} = \frac{E(z)}{1-\nu^2} \qquad Q_{12} = \frac{\nu E(z)}{1-\nu^2} \qquad Q_{44} = Q_{55} = Q_{66} = \frac{E(z)}{2(1+\nu)} \tag{13}$$

2.3.3 Governing equations and boundary conditions

The principle of virtual work in the present case yields

$$\int_{-h/2}^{h/2}\left[\sigma_x\delta\varepsilon_x+\sigma_y\delta\varepsilon_y+\tau_{xy}\delta\gamma_{xy}+\tau_{yz}\delta\gamma_{yz}+\tau_{xz}\delta\gamma_{xz}\right]d\Omega dz+\int_\Omega[f_e\delta w]d\Omega-\int_\Omega q\delta w d\Omega=0 \tag{14}$$

Where Ω is the top surface and q is is the applied transverse load. By substituting Eqs. (10) and (12) into Eq. (14) and integrating through the thickness of the plate, Eq. (14) can be rewritten as

$$\begin{aligned}&\int_\Omega\left[\begin{matrix}N_x\delta\varepsilon_x^0+N_y\delta\varepsilon_y^0+N_{xy}\delta\varepsilon_{xy}^0+M_x^b\delta k_x^b+M_y^b\delta k_y^b+M_{xy}^b\delta k_{xy}^b+M_x^s\delta k_x^s+M_y^s\delta k_y^s\\+M_{xy}^s\delta k_{xy}^s+S_{yz}^s\delta\gamma_{yz}^s+S_{xz}^s\delta\gamma_{xz}^s\end{matrix}\right]d\Omega+\\&+\int_\Omega f_e(\delta w_b+\delta w_s)d\Omega-\int_\Omega q(\delta w_b+\delta w_s)d\Omega=0\end{aligned} \tag{15}$$

Where the stress resultants N, M, and S are defined by

$$\begin{aligned}(N_x,N_y,N_{xy})&=\sum_{n=1}^{3}\int_{h_n}^{h_{n+1}}(\sigma_x,\sigma_y,\tau_{xy})dz\\(M_x^b,M_y^b,M_{xy}^b)&=\sum_{n=1}^{3}\int_{h_n}^{h_{n+1}}(\sigma_x,\sigma_y,\tau_{xy})zdz\\(M_x^s,M_y^s,M_{xy}^s)&=\sum_{n=1}^{3}\int_{h_n}^{h_{n+1}}(\sigma_x,\sigma_y,\tau_{xy})fdz\\(S_{xz}^s,S_{yz}^s)&=\sum_{n=1}^{3}\int_{h_n}^{h_{n+1}}(\tau_{xz},\tau_{yz})gdz\end{aligned} \tag{16}$$

Substituting Eq. (12) into Eq. (16) and integrating through the thickness of the plate, the stress resultants are given as

$$\begin{Bmatrix}N\\M^b\\M^s\end{Bmatrix}=\begin{bmatrix}A&B&B^s\\B&D&D^s\\B^s&D^s&H^s\end{bmatrix}\begin{Bmatrix}\varepsilon\\k^b\\k^s\end{Bmatrix},\qquad\begin{Bmatrix}S_{yz}^s\\S_{xz}^s\end{Bmatrix}=\begin{bmatrix}A_{44}^s&0\\0&A_{55}^s\end{bmatrix}\begin{Bmatrix}\gamma_{yz}^s\\\gamma_{xz}^s\end{Bmatrix} \tag{17}$$

Where

$$N=\{N_x,N_y,N_{xy}\}^t,\quad M^b=\{M_x^b,M_y^b,M_{xy}^b\}^t,\quad M^s=\{M_x^s,M_y^s,M_{xy}^s\}^t \tag{18a}$$

$$\varepsilon=\{\varepsilon_x^0,\varepsilon_y^0,\gamma_{xy}^0\},\quad k^b=\{k_x^b,k_y^b,k_{xy}^b\},\quad k^s=\{k_x^s,k_y^s,k_{xy}^s\} \tag{18b}$$

$$A=\begin{bmatrix}A_{11}&A_{12}&0\\A_{12}&A_{22}&0\\0&0&A_{66}\end{bmatrix},\quad B=\begin{bmatrix}B_{11}&B_{12}&0\\B_{12}&B_{22}&0\\0&0&B_{66}\end{bmatrix},\quad D=\begin{bmatrix}D_{11}&D_{12}&0\\D_{12}&D_{22}&0\\0&0&D_{66}\end{bmatrix} \tag{18c}$$

$$B^s=\begin{bmatrix}B_{11}^s&B_{12}^s&0\\B_{12}^s&B_{22}^s&0\\0&0&B_{66}^s\end{bmatrix},\quad D^s=\begin{bmatrix}D_{11}^s&D_{12}^s&0\\D_{12}^s&D_{22}^s&0\\0&0&D_{66}^s\end{bmatrix},\quad H^s=\begin{bmatrix}H_{11}^s&H_{12}^s&0\\H_{12}^s&H_{22}^s&0\\0&0&H_{66}^s\end{bmatrix} \tag{18d}$$

Where A_{ij}, B_{ij}, etc., are the plate stiffness, defined by

$$A=\begin{bmatrix}A_{11}&B_{11}&D_{11}&B_{11}^s&D_{11}^s&H_{11}^s\\A_{12}&B_{12}&D_{12}&B_{12}^s&D_{12}^s&H_{12}^s\\A_{66}&B_{66}&D_{66}&B_{66}^s&D_{66}^s&H_{66}^s\end{bmatrix}=\int_{-h/2}^{h/2}Q_{11}(1,z,z^2,f(z),zf(z),f^2(z))\begin{Bmatrix}1\\\nu\\\frac{1-\nu}{2}\end{Bmatrix}dz \tag{19}$$

And

$$(A_{22}, B_{22}, D_{22}, B_{22}^{s}, D_{22}^{s}, H_{22}^{s}) = (A_{11}, B_{11}, D_{11}, B_{11}^{s}, D_{11}^{s}, H_{11}^{s})$$
$$A_{44}^{s} = A_{55}^{s} = \int_{h_{n-1}}^{h_n} Q_{44}[g(z)]^2 \, dz \tag{20}$$

And we obtain the following equation,

$$A_{11}\frac{\partial^2 u}{\partial x^2} + A_{66}\frac{\partial^2 u}{\partial y^2} + (A_{12}+A_{66})\frac{\partial^2 v}{\partial x \partial y} - B_{11}\frac{\partial^3 w_b}{\partial x^3} - (B_{12}+2B_{66})\frac{\partial^3 w_b}{\partial x \partial y^2} - B_{11}^{s}\frac{\partial^3 w_s}{\partial x^3} - \left(B_{12}^{s}+2B_{66}^{s}\right)\frac{\partial^3 w_s}{\partial x \partial y^2} = 0 \tag{21a}$$

$$(A_{12}+A_{66})\frac{\partial^2 u}{\partial x \partial y} + A_{66}\frac{\partial^2 v}{\partial x^2} + A_{22}\frac{\partial^2 v}{\partial y^2} - (B_{12}+2B_{66})\frac{\partial^3 w_b}{\partial x^2 \partial y} - B_{22}\frac{\partial^3 w_b}{\partial y^3} - B_{22}^{s}\frac{\partial^3 w_s}{\partial y^3} - \left(B_{12}^{s}+2B_{66}^{s}\right)\frac{\partial^3 w_s}{\partial x^2 \partial y} = 0 \tag{21b}$$

$$B_{11}\frac{\partial^3 u}{\partial x^3} + (B_{12}+2B_{66})\frac{\partial^3 u}{\partial x \partial y^2} + (B_{12}+2B_{66})\frac{\partial^3 v}{\partial x^2 \partial y} + B_{22}\frac{\partial^3 v}{\partial y^3} - D_{11}\frac{\partial^4 w_b}{\partial x^4} - 2(D_{12}+2D_{66})\frac{\partial^4 w_b}{\partial x^2 \partial y^2} - D_{22}\frac{\partial^4 w_b}{\partial y^4} - D_{11}^{s}\frac{\partial^4 w_s}{\partial x^4} - 2\left(D_{12}^{s}+2D_{66}^{s}\right)\frac{\partial^4 w_s}{\partial x^2 \partial y^2} - D_{22}^{s}\frac{\partial^4 w_s}{\partial y^4} - f_e + q = 0 \tag{21c}$$

$$B_{11}^{s}\frac{\partial^3 u}{\partial x^3} + \left(B_{12}^{s}+2B_{66}^{s}\right)\frac{\partial^3 u}{\partial x \partial y^2} + \left(B_{12}^{s}+2B_{66}^{s}\right)\frac{\partial^3 v}{\partial x^2 \partial y} + B_{22}^{s}\frac{\partial^3 v}{\partial y^3} - D_{11}^{s}\frac{\partial^4 w_b}{\partial x^4} - 2\left(D_{12}^{s}+2D_{66}^{s}\right)\frac{\partial^4 w_b}{\partial x^2 \partial y^2} - D_{22}^{s}\frac{\partial^4 w_b}{\partial y^4} - H_{11}^{s}\frac{\partial^4 w_s}{\partial x^4} - 2\left(H_{12}^{s}+2H_{66}^{s}\right)\frac{\partial^4 w_s}{\partial x^2 \partial y^2} - H_{22}^{s}\frac{\partial^4 w_s}{\partial y^4} + A_{55}^{s}\frac{\partial^2 w_s}{\partial x^2} + A_{44}^{s}\frac{\partial^2 w_s}{\partial y^2} - f_e + q = 0 \tag{21d}$$

Since the bottom surface of the plate is subjected to the action of the Winkler-Pasternak elastic foundation, the action-deflection relation at the bottom surface of the model is expressed as

$$f_e = k_0 w - k_1 \nabla^2 w \tag{22}$$

Where f_e is the density of reaction force of the foundation. If the foundation is modeled as a linear Winkler foundation, the coefficient k_1 in Eq. (22) is zero.

3. Navier solution for simply supported rectangular plates

Rectangular plates are generally classified in accordance with the used type support.

We are here concerned with the analytical solutions of Eqs. (21a)-(21d) for the simply supported FG plate. The following boundary conditions are imposed at the side edges.

$$v(-a/2, y) = w_b(-a/2, y) = w_s(-a/2, y) = \frac{\partial w_b}{\partial y}(-a/2, y) = \frac{\partial w_s}{\partial y}(-a/2, y) = 0 \tag{23a}$$

$$v(a/2, y) = w_b(a/2, y) = w_s(a/2, y) = \frac{\partial w_b}{\partial y}(a/2, y) = \frac{\partial w_s}{\partial y}(a/2, y) = 0 \tag{23b}$$

$$N_x(-a/2, y) = M_x^b(-a/2, y) = M_x^s(-a/2, y) = N_x(a/2, y) = M_x^b(a/2, y) = M_x^s(a/2, y) = 0 \tag{23c}$$

$$u(x, -b/2) = w_b(x, -b/2) = w_s(x, -b/2) = \frac{\partial w_b}{\partial x}(x, -b/2) = \frac{\partial w_s}{\partial x}(x, -b/2) = 0 \tag{23d}$$

$$u(x,b/2)=w_b(x,b/2)=w_s(x,b/2)=\frac{\partial w_b}{\partial x}(x,b/2)=\frac{\partial w_s}{\partial x}(x,b/2)=0 \tag{23e}$$

$$N_y(x,-b/2)=M_y^b(x,-b/2)=M_y^s(x,-b/2)=N_y(x,b/2)=M_y^b(x,b/2)=M_y^s(x,b/2)=0 \tag{23f}$$

To solve this problem, Navier assumed that the transverse mechanical and temperature loads, q in the form of a double trigonometric series as

$$q(x,y)=\sum_{m=1}^{\infty}\sum_{n=1}^{\infty} q_{mn}\sin(\lambda x)\sin(\mu y) \tag{24}$$

Where $\lambda = m\pi/a$ and $\mu = n\pi b$ m and n are mode numbers. For the case of a sinusoidal distributed load, we have: $m=n=1$ and $q_{11}=q_0$

$$q(x,y)=q_0\sin(\lambda x)\sin(\mu y) \tag{25}$$

q_0 represents the intensity of the load at the plate center. Following the Navier solution procedure, we assume the following solution form for u, v, w_b, w_s that satisfies the boundary conditions, The displacement functions that satisfy the equations of boundary conditions Eq. (26) are selected as the following Fourier series

$$\begin{Bmatrix} u \\ v \\ w_b \\ w_s \end{Bmatrix}=\sum_{m=1}^{\infty}\sum_{n=1}^{\infty}\begin{Bmatrix} U_{mn}\cos(\lambda x)\sin(\mu y) \\ V_{mn}\sin(\lambda x)\cos(\mu y) \\ W_{bmn}\sin(\lambda x)\sin(\mu y) \\ W_{smn}\sin(\lambda x)\sin(\mu y) \end{Bmatrix} \tag{26}$$

Where U_{mn}, V_{mn}, W_{bmn}, and W_{smn} are arbitrary parameters to be determined subjected to the condition that the solution in Eq. (26) satisfies governing Eq. (21). Eq. (26) reduces the governing equations for flexural analysis to the following form

$$[C]\{\Delta\}=\{P\} \tag{27}$$

Where

$$\{\Delta\}=\{U_{mn},V_{mn},\mathrm{W}_{\mathrm{bmn}},\mathrm{W}_{\mathrm{smn}}\}^t \tag{28}$$

$$\{P\}=\{0,0,-q_{mn},-q_{mn}\}^t \tag{29}$$

And (c) is the symmetric matrix given by

$$[C]=\begin{bmatrix} a_{11} & a_{12} & a_{13} & a_{14} \\ a_{12} & a_{22} & a_{23} & a_{24} \\ a_{13} & a_{32} & a_{33} & a_{34} \\ a_{14} & a_{42} & a_{43} & a_{44} \end{bmatrix} \tag{30}$$

In which

$$\begin{aligned} a_{11} &= -(A_{11}\lambda^2 + A_{66}\mu^2) \\ a_{12} &= -(\lambda\,\mu\,(A_{12}+A_{66})) \\ a_{13} &= -\lambda\,[B_{11}\lambda^2 + (B_{12}+2B_{66})\,\mu^2] \\ a_{14} &= -\lambda\,[B_{11}^s\lambda^2 + (B_{12}^s+2B_{66}^s)\,\mu^2] \end{aligned} \tag{31}$$

$$a_{22} = -(A_{66}\lambda^2 + A_{22}\mu^2)$$
$$a_{23} = \mu[(B_{12} + 2B_{66})\,\lambda^2 + B_{22}\mu^2]$$
$$a_{24} = -\mu[(B_{12}^s + 2B_{66}^s)\,\lambda^2 + B_{22}^s\mu^2]$$
$$a_{33} = D_{11}\lambda^4 + 2(D_{12} + 2D_{66})\lambda^2\mu^2 + D_{22}\mu^4 + k_1(\lambda^2 + \mu^2) + k_0$$
$$a_{34} = D_{11}^s\lambda^4 + 2(D_{12}^s + 2D_{66}^s)\lambda^2\,\mu^2 + D_{22}^s\,\mu^4$$
$$a_{44} = H_{11}^s\lambda^4 + 2(H_{12}^s + 2H_{66}^s)\lambda^2\mu^2 + H_{22}^s\mu^4 + A_{55}^s\lambda^2 + A_{44}^s\mu^2 - k_1(\lambda^2 + \mu^2) + k_0$$

4. Results and discussion

In numerical analysis, dimensionless deflection and stresses of simply supported perfect and imperfect FG Plates resting on the foundations elastic are evaluated. The FG plate is taken to be made of aluminum and alumina with the following material properties

Ceramic (P_c: Alumina, Al_2O_3): E_c=380 Gpa; v=0.3; ρ=2702 kg/m^3

Metal (P_m: Aluminium, Al): E_m=70 Gpa; v=0.3; ρ=5700 kg/m^3

And their properties change through the thickness of the plate according to power-law. The bottom surfaces of the FG plate are aluminum rich, whereas the top surfaces of the FG plate are alumina rich.

For convenience, the following dimensionless form is used

$$\bar{w} = 10\frac{E_C h^3}{q_0 a^4} w\left(\frac{a}{2},\frac{b}{2}\right),\quad \bar{u} = 100\frac{E_C h^3}{q_0 a^4} u\left(0,\frac{b}{2},\frac{-h}{4}\right),\quad \bar{v} = 100\frac{E_C h^3}{q_0 a^4} v\left(\frac{a}{2},0,\frac{-h}{6}\right),\quad \bar{\sigma}_x = \frac{h}{hq_0}\sigma_x\left(\frac{a}{2},\frac{b}{2},\frac{h}{2}\right),\quad \bar{\sigma}_y = \frac{h}{hq_0}\sigma_y\left(\frac{a}{2},\frac{b}{2},\frac{h}{3}\right),$$
$$\bar{\tau}_{xy} = \frac{h}{hq_0}\tau_{xy}\left(0,0,-\frac{h}{3}\right),\quad \bar{\tau}_{xz} = \frac{h}{hq_0}\tau_{xz}\left(0,\frac{b}{2},0\right),\quad \bar{\tau}_{yz} = \frac{h}{hq_0}\tau_{yz}\left(\frac{a}{2},0,\frac{h}{6}\right).$$

To validate accuracy of the two refined plate theory, the comparisons between the present results and the available results obtained by Kobayashi *et al*. (1989), Lam *et al*. (2000), Benyoucef *et al*. (2008), Karama (2003), Zenkour (2006), and Reddy (1984). The two present solutions are realized for a square plate on a Winkler Foundation while Winkler modulus is considered to vary from 1 to 5^4 in Table 1. It is to be noted that the present results of the Deflection compare very well with the other theories solution for perfect FG plate (α=0) and takes larger values for the imperfect FG plate (α=0.1 and α=0.2). This is expected because the imperfect FG plate is the one with the lowest stiffness and the perfect FG plate is the one with the highest stiffness.

Table 1 Effect of volume fraction of porosity on the deflection of a uniformly loaded simply supported homogeneous square plate on a Winkler foundation

K_0	Dw(0.5a, 0.5a)/qa^4.10^3								
	Kobayashi (1989)	Lam (2000)	Benyoucef (2010)	Present Theory 1			Present Theory 2		
	α=0	α=0	α=0	α=0 (Benferhat 2015)	α=0.1	α=0.2	α=0 (Daouadji 2012)	α=0.1	α=0.2
1	4.052	4.053	4.053	4.053803	4.308226	4.596725	4.053804	4.308228	4.596726
3^4	3.347	3.349	3.348	3.348534	3.520069	3.710100	3.348535	3.520070	3.710101
5^4	1.506	1.507	1.506	1.506099	1.537886	1.570776	1.506098	1.537886	1.570776

Table 2 Effect of volume fraction of porosity on the center deflections of a uniformly loaded simply supported homogeneous square plate (a/h=100) on Winkler-Pasternak foundation

K_0	K_1	$Dw(0.5a, 0.5a)/qa^4.10^3$						
		Lam (2000)	Present Theory 1			Present Theory 2		
		α=0	α=0 (Benferhat 2015)	α=0.1	α=0.2	α=0 (Daouadji 2012)	α=0.1	α=0.2
1	1	3.853	3.855024	4.084390	4.342776	3.855024	4.084391	4.342777
	3^4	0.763	0.762973	0.7708801	0.7789082	0.7629731	0.7708801	0.7789082
	5^4	0.115	0.115304	0.1154558	0.1156074	0.1153043	0.1154558	0.1156074
3^4	1	3.210	3.210791	3.368101	3.541586	3.210791	3.368102	3.541587
	3^4	0.732	0.731729	0.7389251	0.7462183	0.7317292	0.7389251	0.7462184
	5^4	0.115	0.114524	0.1146730	0.1148219	0.1145241	0.1146730	0.1148219
5^4	1	1.476	1.476523	1.507000	1.538500	1.476523	1.507001	1.53850
	3^4	0.570	0.570364	0.5743668	0.5783767	0.5703637	0.5743668	0.5783767
	5^4	0.109	0.109471	0.1096031	0.1097352	0.1094709	0.1096031	0.1097352

The center deflections of a uniformly loaded simply supported homogeneous perfect and imperfect square plate resting on elastic foundations with different values of K_0 and K_1 are computed in Table 2. It can be seen that the center deflections of this study show a satisfied agreement with those obtained by Lam *et al*. (2000) for the perfect FG square plates with various values of K_0 and K_1. In addition the comparisons show that the effect of the porosity on the center deflections of FG plates with two different type of porosity. The results reveal that center deflections results increase as the volume fraction of porosity (a) increases. In Table 3, the effects of volume fraction of porosity, side-to-thickness ratio and elastic foundation parameters on the dimensionless center deflection and stresses of anisotropic square plate with or without the porosity is given. It is clear that with increasing of the side-to thickness ratio a/h the center deflection w decrease and the stresses increase. However, the center deflection w increase and the stresses decrease with the existence of the porosity (α=0.1 and α=0.2). As observed in these results there is a very good agreement between the two present new trigonometric shear deformation plate

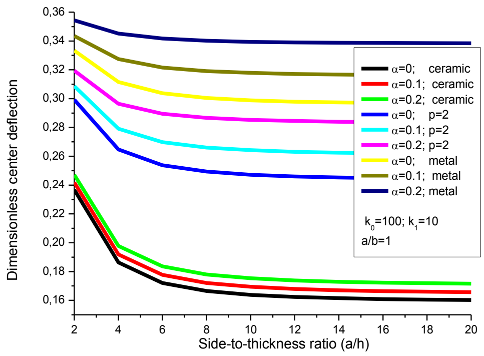

Fig. 2 Effect of volume fraction of porosity on the dimensionless center deflection versus side-to-thickness ratio a/h of an FGM square plate on elastic foundations

Table 3 Effect of side-to-thickness ratio and elastic foundation parameters on the dimensionless deflection and stresses of an isotropic square perfect and imperfect FGM plate

a/*h*	K_0	K_1	Theories	α	*w*	σ_x	τ_{xy}	τ_{xz}
10	100	10	Karama (2003)	α=0	0.1638744	1.105538	0.3911440	0.1405294
			Zenkour (2006)	α=0	0.1638971	1.104803	0.3911620	0.1362969
			Reddy (1984)	α=0	0.1639048	1.104109	0.3912240	0.1320798
			Present Theory 1	α=0 (Benferhat 2015)	0.1638971	1.1048037	0.3911618	0.1362969
				α=0.1	0.1694520	1.074615	0.3804734	0.1325727
				α=0.2	0.1753967	1.042309	0.3690352	0.1285871
			Present Theory 2	α=0 (Daouadji 2012)	0.1639008	1.104590	0.3911785	0.1351198
				α=0.1	0.1694558	1.074406	0.3804895	0.1314277
				α=0.2	0.1754005	1.042106	0.3690505	0.1274765
50	100	10	Karama (2003)	α=0	0.1591473	5.599530	2.008916	0.1439351
			Zenkour (2006)	α=0	0.1591483	5.599378	2.008920	0.1395914
			Reddy (1984)	α=0	0.1591486	5.599238	2.008934	0.1352572
			Present Theory 1	α=0 (Benferhat 2015)	0.1591482	5.5993809	2.0089210	0.1395915
				α=0.1	0.1646725	5.450695	1.955576	0.1358847
				α=0.2	0.1705942	5.291317	1.898395	0.1319115
			Present Theory 2	α=0 (Daouadji 2012)	0.1591483	5.599337	2.008924	0.1383820
				α=0.1	0.1646727	5.450653	1.955579	0.1347075
				α=0.2	0.1705944	5.291275	1.898398	0.1307686
100	100	10	Karama (2003)	α=0	0.1589959	11.20366	4.021240	0.1440442
			Zenkour (2006)	α=0	0.1589961	11.20359	4.021243	0.1396969
			Reddy (1984)	α=0	0.1589962	11.20353	4.021248	0.1353590
			Present Theory 1	α=0 (Benferhat 2015)	0.1589961	11.2035895	4.0212443	0.1396969
				α=0.1	0.1645193	10.90636	3.914564	0.1359909
				α=0.2	0.1704401	10.58775	3.800205	0.1320181
			Present Theory 2	α=0 (Daouadji 2012)	0.1589961	11.20356	4.021246	0.1384865
				α=0.1	0.1645194	10.90634	3.914565	0.1348126
				α=0.2	0.1704402	10.58773	3.800207	0.1308742

theory and other higher order plate theories.

Fig. 2 depicts the variation of the dimensionless center deflection $\bar{w}$ through side-to-thickness ratio with the variations of the volume fraction exponent (ceramic, *P*=2 and metal) and the volume fraction of the porosity (α=0.1 and α=0.2). It is seen that the results are the maximum for the metal and for the imperfect plates and the minimum for the ceramic and the perfect plates. This is expected because the imperfect metallic plate is the one with the lowest stiffness and the perfect ceramic plate is the one with the highest stiffness.

Fig. 3 show the variation of the In-plane longitudinal stress $\bar{\sigma}_x$ through the thickness and from

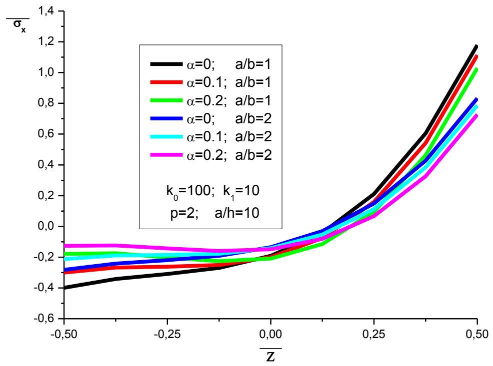

Fig. 3 Effect of volume fraction of porosity on the in-plane longitudinal stress through the thickness of an FGM plate

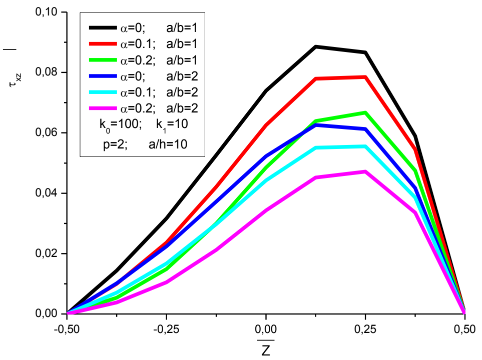

Fig. 4 Effect of volume fraction of porosity on the transversal shear stress through-the thickness

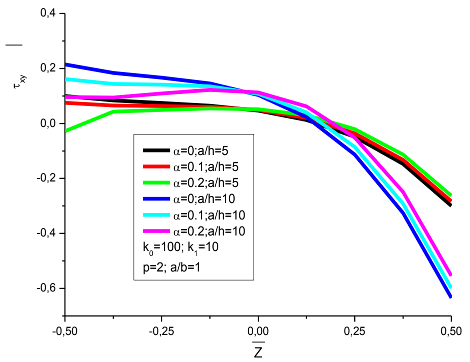

Fig. 5 Effect of volume fraction of porosity on the longitudinal tangential stress through-the thickness of an FGM plate

the aspect ratio *a*/*b* of a perfect and imperfect FG plates on elastic foundations based on the present plate theory. The volume fraction exponent of the FG plate in taken as *P*=2. It's clear that the stresses are tensile at the top surface and compressive at the bottom surface and take the minimum values for the imperfect FG plate. Figs. 4 and 5 contains the plots of the transversal shear stress $\bar{\tau}_{xz}$ and the longitudinal tangential stress $\bar{\tau}_{xy}$ through-the thickness with the different values of the aspect and side-to-thickness ratio, respectively.

As illustrated in Fig. 4, the distributions of the transversal shear stress $\bar{\tau}_{xz}$ are not parabolic and decreases gradually with increasing of the volume fraction of the porosity and the aspect ratio. Contrary to the in-plane longitudinal normal stress $\bar{\sigma}_x$, the magnitude of the tangential stress $\bar{\tau}_{xy}$ is maximum at points on the bottom and top surfaces of the FGM plate and it can be seen that $\bar{\tau}_{xy}$ take the minimum value for the FG plate with increasing of the volume fraction of the porosity.

5. Conclusions

The effect of the porosity on the bending analysis for the advanced composite plate resting on the elastic foundations is presented. Parametric study in this analysis is being carried out. These parameters include (i) power-law index, (ii) the aspect ratio, (iii) side-to-thickness ratio, (iv) variable Winkler foundation modulus, (v) two-parameter elastic foundation modulus and (vi) the volume fraction of the porosity.

Present results for the perfect FG plate with Winkler and two-parameter elastic foundations based on the two present plate theories do agree with those reported in the literature. The modified rule of mixture covering porosity phases is used to describe and approximate material properties of the imperfect FG plates. The influence of the porosities on the dimensionless center deflection and stresses is then discussed. It’s to be noted that with increasing of the volume fraction of the porosity the dimensionless center deflection increase and the stresses decrease. All comparison studies demonstrate that the present solution is highly efficient for the exact analysis of the bending of FG plates. In conclusion, it can be said that the two proposed theories are accurate and simple in solving the analysis of FG plates on the elastic foundations.

Acknowledgments

The authors thank the referees for their valuable comments.

References

Abdelhak Z., Hadji, L, Daouadji, T.H. and Bedia, E.A. (2015), “Thermal buckling of functionally graded plates using an-order four variable refined theory”, *Adv. Mater. Res.*, **4**(1), 31-44.

Adim, B., Hassaine D.T. and Rabahi A. (2016), “A simple higher order shear deformation theory for mechanical behavior of laminated composite plates”, *J. Adv. Struct. Eng.*, **8**(2), 103-117.

Meziane, M.A.A., Abdelaziz, H.H. and Tounsi, A. (2015), “An efficient and simple refined theory for buckling and free vibration of exponentially graded sandwich plates under various boundary conditions”, *J. Sandwich Struct. Mater.*, **16**(3), 293-318.

Baghdadi, H., Tounsi, A., Zidour, M. and Benzair, A. (2015), “Thermal effect on vibration characteristics of armchair and zigzag single-walled carbon nanotubes using nonlocal parabolic beam theory”, *Nanotub. Carbon Nanostruct.*, **23**(3), 266-272.

Bellifa, H., Benrahou, K., Houari, S.A. and Tounsi, A. (2015), “Bending and free vibration analysis of functionally graded plates using a simple shear deformation theory and the concept the neutral surface position”, *J. Brazil. Soc. Mech. Sci. Eng.*, **38**(1), 265-275.

Benferhat, R., Daouadji, T.H. and Mansour, M.S. (2015), “A higher order shear deformation model for bending analysis of functionally graded plates", *Trans. Indian Institut. Metals.*, **68**(1), 7-16.

Bensattalah, T., Zidour, M., Tounsi, A. and Bedia, E.A.A. (2016), "Investigation of thermal and chirality effects on vibration of single-walled carbon anotubes embedded in a polymeric matrix using nonlocal elasticity theories", *Mech. Compos. Mater.*, **52**(4), 1-14.

Benyoucef, S., Mechab, I., Tounsi, A., Fekrar, A., Ait, A.H., Adda, B.E. (2010), "Bending of thick functionally graded plates resting on winkler-pasternak elastic foundations", *Mech. Compos. Mater.*, **46**(4), 425-434.

Bouazza, M., Amara, K., Zidour, M., Tounsi, A. and Adda, B.E. (2015), "Postbuckling analysis of functionally graded beams using hyperbolic shear deformation theory", *Rev. Informat. Eng. Appl.*, **2**(1), 1-14.

Bouazza, M., Amara, K., Zidour, M., Tounsi, A. and Adda, B.E. (2015), "Postbuckling analysis of nanobeams using trigonometric Shear deformation theory", *Appl. Sci. Rep.*, **10**(2), 112-121.

Bouazza, M., Amara, K., Zidour, M., Tounsi, A. and Adda, B.E. (2014), "Hygrothermal effects on the postbuckling response of composite beams", *Am. J. Mater. Res.*, **1**(2), 35-43.

Boumia, L., Zidour, M., Benzair, A. and Tounsi, A. (2014), "A timoshenko beam model for vibration analysis of chiral single-walled carbon nanotubes", *Phys. E: Low-dimens. Syst. Nanostruct.*, **59**, 186-191.

Bourada, M., Kaci, A., Houari, S.A. and Tounsi, A. (2015), "A new simple shear and normal deformations theory for functionally graded beams", *Steel Compos. Struct.*, **18**(2), 409-423.

Chakraborty, A., Gopalakrishnan, S. and Reddy, J.N. (2003), "A new beam finite element for the analysis of functionally graded materials", *J. Mech. Sci.*, **45**(3), 519-539.

Gafour, F., Zidour, M., Tounsi, A., Heireche, H. and Semmah, A. (2015), "Sound wave propagation in zigzag double-walled carbon nanotubes embedded in an elastic medium using nonlocal elasticity theory", *Phys. E: Low-dimens. Syst. Nanostruct.* **48**, 118-123.

Hamidi, A., Houari, S.A., Mahmoud, S.R. and Tounsi, A. (2015), "A sinusoidal plate theory with 5-unknowns and stretching effect for thermomechanical bending of functionally graded sandwich plates", *Steel Compos. Struct.*, **18**(1), 235-253.

Daouadji, T.H., Hadji, L., Hadji, A., Henni, A.H. and El Abbes, A.B. (2012), "A theoretical analysis for static and dynamic behavior of functionally graded plates", *Mater. Phys. Mech.*, **14**(2), 110-128.

Daouadji, T.H., Benferhat, R. and Adim B. (2016), "A novel higher order shear deformation theory based on the neutral surface concept of FGM plate under transverse load", *Adv. Mater. Res.*, **5**(2), 107-123.

Daouadji, T.H. and Tounsi, A. (2013), "Analytical solution for bending analysis of functionally graded plates", *Sci. Iran., Trans. B: Mech. Eng.*, **20**(3), 516-523.

Daouadji T.H., Henni, A.H., Tounsi, A. and El Abbes, A.B. (2013), "Elasticity solution of a cantilever functionally graded beam", *Appl. Compos. Mater.*, **20**(1), 1-15.

Karama, M., Afaq, K.S. and Mistou, S. (2003), "Mechanical behaviour of laminated composite beam by new multi-layered laminated composite structures model with transverse shear stress continuity", *J. Solids Struct.*, **40**(6), 1525-1546.

Kerr, A.D. (1964), "Elastic and viscoelastic foundation models", *ASME J. Appl. Mech.*, **31**(3), 491-498.

Kobayashi, H. and Sonoda, K. (1989), "Rectangular mindlin plates on elastic foundations", *J. Mech. Sci.*, **31**(9), 679-692.

Koizumi, M. (1992), "The concept of FGM", **34**, 3-10.

Koizumi, M. (1997), "FGM activities in Japan", *Compos. Part B: Eng.*, **28**(1-2), 1-4.

Lam, K.Y., Wang, C.M. and He, X.Q. (2000), "Canonical exact solutions for Levy-plates on two-parameter foundation using Green's functions", *Eng. Struct.*, **22**(4), 364-378.

Mahi, A. and Tounsi, A. (2015), "A new hyperbolic shear deformation theory for bending and free vibration analysis of isotropic, functionally graded, sandwich and laminated composite plates", *Appl. Math. Model.*, **39**(9), 2489-2508.

Mantari, J.L. and Soares, C.G. (2014), "A trigonometric plate theory with 5-unknowns and stretching effect for advanced composite plates", *Compos. Struct.*, **107**, 396-405.

Meksi, A., Benyoucef, S., Houari, M.S.A. and Tounsi, A. (2015), "A simple shear deformation theory based on neutral surface position for functionally graded plates resting on Pasternak elastic foundations", *Struct.*

Eng. *Mech*., **53**(6), 1215-1240.
Naceri, M., Zidour, M., Semmah, A., Houari, M.S.A., Benzair, A. and Tounsi, A. (2012), “Sound wave propagation in armchair single walled carbon nanotubes under thermal environment”, *J*. *Appl*. *Phys*., **110**(12), 124-132.
Pasternak, P.L. (1954), *On a New Method of Analysis of an Elastic Foundation by Means of Two Foundation Constants*, Gosudarstvennoe Izdatelstvo Literaturi Po Stroitelstvu I Arkhitekture, Moscow, Russia.
Pradhan, S.C. and Murmu, T. (2009), “Thermo-mechanical vibration of FGM sandwich beam under variable elastic foundations using differential quadrature method”, *J*. *Sound Vibr*., **321**(1), 342-362.
Reddy, J.N. (1984), “A simple higher-order theory for laminated composite plates”, *J*. *Appl*. *Mech*., **51**(4), 745-752.
Shen, H.S. and Wang, Z.X. (2010), “Nonlinear bending of FGM plates subjected to combined loading and resting on elastic foundations”, *Compos*. *Struct*., **92**(10), 2517-2524.
Suresh, S. and Mortensen, A. (1998), *Fundamentals of Functionally Graded Materials*, IOM Communications, London, U.K.
Tlidji, Y., Daouadji T.H., Hadji, L., Tounsi, A. and Bedia E.A.A. (2014), “Elasticity solution for bending response of functionally graded sandwich plates under thermo mechanical loading”, *J*. *Therm*. *Stress*., **37**(7), 852-869.
Wattanasakulpong, N., Prusty, B.G., Kelly, D.W. and Hoffman, M. (2012), “Free vibration analysis of layered functionally graded beams with experimental validation”, *Mater*. *Des*., **36**, 182-190.
Wattanasakulpong, N. and Ungbhakorn, V. (2014), “Linear and nonlinear vibration analysis of elastically restrained ends FGM beams with porosities”, *Aero*. *Sci*. *Technol*., **32**(1), 111-120.
Xiang, Y., Wang, C.M. and Kitipornchai, S. (1994), “Exact vibration solution for initially stressed mindlin plates on pasternak foundation”, *J*. *Mech*. *Sci*., **36**(4), 311-316.
Zenkour, A.M. (2006), “Generalized shear deformation theory for bending analysis of functionally graded materials”, *Appl*. *Math*. *Model*., **30**(1), 67-84.
Zenkour, A.M. (2010), “Hygro-thermo-mechanical effects on FGM plates resting on elastic foundations”, *Compos*. *Struct*., **93**(1), 234-238.
Zhou, D., Cheung, Y.K., Lo, S.H. and Au, F.T.K. (2004), “Three-dimensional vibration analysis of rectangular thick plates on pasternak foundations”, *J*. *Numer*. *Methods Eng*., **59**(10),1313-1334.
Zhu, J., Lai, Z., Yin, Z., Jeon, J. and Lee, S. (2001), “Fabrication of ZrO2-NiCr functionally graded material by powder metallurgy”, *Mater*. *Chem*. *Phys*., **68**(1), 130-135.
Zidour, M., Benrahou, K.H., Tounsi, A., Bedia, E.A.A. and Hadji, L. (2014), “Buckling analysis of chiral single-walled carbon nanotubes by using the nonlocal timoshenko beam theory”, *Mech*. *Compos*. *Mater*., **50**(1), 95-104.

AI